Cancer Gene Therapy (2009) 16, 848–860
 0929-1903/09 $32.00
www.nature.com/cgt

ORIGINAL ARTICLE

Adenovirus delivery of human CD40 ligand gene confers direct therapeutic effects on carcinomas

L Vardouli[1], C Lindqvist[2], K Vlahou[1], ASI Loskog[2] and AG Eliopoulos[1,3]

[1]*Molecular and Cellular Biology Laboratory, Division of Basic Sciences, University of Crete Medical School, Heraklion, Crete, Greece;* [2]*Rudbeck Laboratory, Clinical Immunology Division, Uppsala University, Uppsala, Sweden and* [3]*Institute for Molecular Biology and Biotechnology, Foundation of Research and Technology Hellas, Heraklion, Crete, Greece*

CD40, a tumor necrosis factor receptor family member, is an emerging target for cancer therapy being best appreciated as an important regulator of the anti-tumor immune response. In this study, we report the development of a replication-defective recombinant adenovirus (RAd) vector expressing human CD40 ligand (RAd-hCD40L) and show that sustained engagement of the CD40 pathway in malignant cells results in direct anti-proliferative and pro-apoptotic effects. Thus, transduction of CD40-positive bladder, cervical and ovarian carcinoma cell lines with RAd-hCD40L potently inhibits their proliferation *in vitro,* whereas CD40-negative lines remain unresponsive. RAd-hCD40L is also found to be superior to recombinant CD40L in inducing carcinoma cell death and in amplifying the cytotoxic effects of the chemotherapeutic agents 5-fluorouracil, *cis*-platin and mitomycin C. Soluble CD40L is produced by RAd-hCD40L transduced carcinoma cells but unlike other soluble tumor necrosis factor family ligands, it does not interfere with the death-promoting activity of its membrane-bound form. In a mouse xenograft tumor model bearing a human bladder carcinoma, intratumoral delivery of RAd-hCD40L suppresses cancer growth. These findings highlight the potential of exploiting the CD40 pathway in carcinomas using CD40L gene transfer alone or in combination with other modalities for cancer therapy. Our results have also broader implications in understanding the multifaceted anti-tumor activities of the CD40 pathway in carcinomas, which thus offer an attractive option for future clinical application.
Cancer Gene Therapy (2009) **16,** 848–860; doi:10.1038/cgt.2009.31; published online 22 May 2009

Keywords: CD40; CD154; gene therapy; carcinoma; apoptosis; adenovirus

Introduction

CD40 is a member of the tumor necrosis factor (TNF) receptor superfamily with a prominent role in immune regulation and homeostasis.[1,2] Indeed, the interaction of CD40 expressed on B lymphocytes with the CD40 ligand (CD40L, CD154), which is found predominantly on activated T cells, is critical for the induction of adaptive immunity by promoting proliferation and differentiation of B lymphocytes into immunoglobulin-producing plasma cells. CD40 is also expressed on other lymphoid cell types, such as macrophages and dendritic cells (DCs) in which its activation contributes to antigen presentation and the production of cytokines that influence T-cell priming and the innate immune response to a variety of extracellular and intracellular pathogens.[2] Of note, activation of CD40 on DCs stimulates strong IL-12 production that is required for efficient engagement of cytotoxic T lymphocyte (CTL) responses and generation of protective anti-tumor immunity.[3]

The latter observation highlights the potential of using CD40L for cancer immunotherapy. Concomitant with this idea, a number of reports have showed that CD40L stimulates a dendritic cell-mediated Th1 anti-tumor immune response, which suppresses cancer growth in the absence of CD40 expression on the malignant cells.[4–6] Thus, recombinant adenovirus (RAd)-mediated delivery of murine CD40L to syngeneic mouse models carrying CD40-negative colorectal, lung or bladder carcinomas results in sustained tumor regression.[7,8] The role of immune cells in this effect has been confirmed by infecting DCs *ex vivo* with murine RAd-CD40L and inoculating them into the subcutaneous tumors. This approach not only eradicated the primary tumor nodule but also protected against subsequent tumor challenge. Importantly, CD40L gene therapy also counteracts immune escape mechanisms by suppressing regulatory T-cell function and promoting the maturation of DCs in the tumor microenvironment.[6,9]

The expression of CD40 is, however, not restricted to immune cells. High levels of CD40 are detected in a wide range of human carcinomas, including those of the ovary,

Correspondence: Professor AG Eliopoulos, Division of Basic Sciences, The University of Crete Medical School, Voutes, Heraklion, Crete 71003, Greece. E-mail: eliopag@med.uoc.gr
Received 8 August 2008; revised 28 November 2008; accepted 23 January 2009; published online 22 May 2009

liver, lung, cervix, bladder and breast.[10,11] Experimental observations demonstrate that the stimulation of CD40 on human carcinoma cells by recombinant soluble (rs) CD40L results in suppression of tumor cell proliferation *in vitro*[12,13] and in xenotransplanted mouse models.[14,15] CD40 engagement may also decrease the viability of carcinoma cells in the presence of protein synthesis inhibitors or antagonists of the anti-apoptotic PI3-kinase/mammalian target of rapamycin signaling pathway.[16–18] Interestingly, apoptosis induced by CD40L in carcinoma cells occurs independently of the p53 tumor suppressor,[19] which is frequently inactivated in cancer, and of the nuclear factor-κB pathway that is constitutively engaged in a plethora of human tumors and influences their response to chemotherapy.[20]

The aforementioned direct effects of CD40L on the proliferation and survival of CD40-positive carcinoma cells coupled with its ability to potentiate anti-tumor immune responses suggest that the CD40 pathway can be exploited for the treatment of solid tumors.[21–23] This is supported by a recent phase I clinical trial of systemic administration of rsCD40L protein, which resulted in remission in a patient with a CD40-positive advanced laryngeal cancer.[24] The therapeutic benefit of soluble CD40L is, however, hindered by its relatively high *in vivo* turnover rate.[24] In this study, we evaluate the concept that delivery of human CD40L to malignant cells by an RAd improves its CD40 stimulatory capacity and enhances the direct pro-apoptotic effects of this pathway on human carcinomas.

Materials and methods

Cell lines and culture

The human cervical carcinoma cell lines CaSki and HeLa and the bladder carcinoma cell line EJ were cultured in RPMI supplemented with 10% FBS. The bladder carcinoma cell lines T24 and VM-CUB1 were cultured in DMEM supplemented with 10% FBS. On the basis of human leukocyte antigen (HLA) type and enzyme studies, O'Toole *et al*.[25] reported that EJ cells are identical to T24. Nevertheless, the two lines differ in various biological properties including tumorigenicity, with only EJ being able to form tumors in nude mice.[26] In agreement with the latter report, the T24 cells used in our study do not form subcutaneous tumors in immunodeficient mice (data not shown). Moreover, T24 were found to express higher levels of CD40 (Table 1). AGE60 is an ovarian carcinoma line generated in our laboratory from the ascitic fluid of a 60-year-old patient with epithelial adenocarcinoma of the ovary. Briefly, the cell pellet obtained from the ascetic fluid was re-suspended in DMEM and live cells were separated from dead cells and erythrocytes by centrifugation on Ficoll-Hypaque (Nycomed Pharma, Norway). Tumor cells were then separated from mononuclear cells by centrifugation on 75–100% discontinuous Ficoll-Hypaque gradients. Tumor cells were expanded in DMEM supplemented with 10% FCS, 1% non-essential aminoacids, 10 μg ml^{-1} insulin and 1% penicillin/streptomycin. All cell culture media were purchased from Invitrogen Corp., AntiSel Bros, Thessaloniki, Greece.

Table 1 CD40 expression levels in human carcinoma (Cx) cell lines

Tumor cell line	*MFI*[a]	*% Positive cells*
EJ bladder Cx	21.3	>98%
T24 bladder Cx	55.2	>98%
VM-CUB1 bladder Cx	38.6	>98%
HeLa cervical Cx	1 (−ve)	N/A
HeLa/CD40 cervical Cx	2.3	85%
CaSki cervical Cx	6.5	90%
AGE60 ovarian Cx	20.4	>98%

[a]MFI, mean fluorescence intensity.

Recombinant adenoviruses and viral transduction

Three replication-deficient, E1/E3-deleted human adenoviruses (type 5) were produced using the AdEasy XL adenoviral vector system (Stratagene, La Jolla, CA), according to the manufacturer's protocol. The RAd-hCD40L and RAd-hmutCD40L viruses code for the human CD40L molecule in its wild type or the $C^{194} \rightarrow W$-mutated form, respectively. The RAd-LacZ is a control virus expressing β-galactosidase. To generate CD40L-expressing RAds, the hCD40L was PCR amplified from activated T lymphocyte cDNA and cloned into pShuttle-CMV (cytomegalovirus) vector as a NotI/*Eco*RV product. Shuttle plasmids were homologously recombined with pAdEasy 1 in BJ5183 bacteria (Stratagene) to generate RAd DNA. Adenoviruses were produced by four rounds of infection of Ad-293 cells (Stratagene). Virus titers were determined by a fluorescence forming unit (f.f.u.) assay that has been verified to give comparable titers to a standard plaque-forming units assay.[27] Briefly, 911 cells were plated on collagen-coated 35 mm plates with grids (Sarstedt, Numbrect, Germany) and infected with purified virus at various dilutions. Cells were cultured for 48 h, washed with PBS, fixed in 4% paraformaldehyde, washed once with PBS and once with PBS with 0.05% Tween-20 and incubated with a mouse monoclonal anti-adenovirus antibody (MAB8052, Chemicon, Temecula, CA) diluted 1:250 in PBS for 1 h at RT. Cells were washed twice with PBS and once with PBS with Tween-20 and incubated for 1 h with a secondary Oregon Green-488 labelled anti-mouse antibody (Molecular Probes, Invitrogen, AntiSel O.E, Greece) diluted 1:1000 in PBS. Fluorescent cells were counted using a Leica DMIRE2 inverted phase contrast microscope with a fluorescence illuminator (Leica, Microsystems, Wetzlar, Germany).

Unless otherwise noted, the human cell lines were transduced with adenoviruses in media containing 2% FBS at a multiplicity of infection (MOI) of 100 for EJ, 25 for T24, 100 for VM-CUB1, 10 for CaSki, 10 for HeLa and MOI 10 for AGE60. Under these conditions approximately 70–80% of the infected cells expressed CD40L. Three hours after transduction, the medium was replaced with fresh 2% FBS medium with or without chemotherapeutics and the cells were incubated for further 24–48 h before analysis.

Flow cytometry and detection of soluble CD40L

CD40L or CD40 expression were determined by flow cytometry using a FITC-conjugated CD154 Ab diluted at 1:25 or supernatant from the murine anti-CD40 hybridoma G28.5 diluted at 1:50. For CD40 expression in cells an additional step included a light protected incubation with a FITC-conjugated anti-mouse Ab (1:500 dilution). Appropriate FITC-conjugated isotype control was used to measure background staining. For cell-cycle analysis by flow cytometry, cells were lightly trypsinized, left to recover in complete medium for 20 min, washed and re-suspended in 1 ml of a 1:1 mixture of PBS and McIlvaine's buffer (0.2 M Na_2PO_4, 0.1 M citric acid, pH: 7.5). Two volumes of ice cold absolute ethanol were added with light vortexing of samples to fix cells that were then incubated at 4 °C for 1 h, washed once with ddH_2O and re-suspended in propidium iodide (PI) staining solution (PBS containing 100 μg ml^{-1} RNAseA and 10 μg ml^{-1} PI). Cells were incubated for 1 h at 4 °C then centrifuged to discard supernatant and re-suspended in 500 μl fresh staining solution. Samples were analyzed immediately by flow cytometry. To detect and quantify soluble hCD40L secreted by the virally transduced cells, the human CD40L ELISA detection kit (Bender MedSystems Inc., Burlingame, CA) was used according to the manufacturer's instructions.

Antibodies and immunoblotting

The anti-caspase-8 and anti-caspase-9 (1/500 dilution) Abs were from Cell Signaling Technology, Beverly, MA. The mouse monoclonal anti-CD154 Ab (1/500 dilution) was purchased from Santa Cruz Biotechnology, Santa Cruz, CA and the mouse-monoclonal anti-β-tubulin Ab (1/2000 dilution) was from Sigma-Aldrich, St Louis, Missouri. The anti-ERK1 Ab (1/1000 dilution) was purchased from Santa Cruz. Anti-rabbit IgG HRP (1/100 000 dilution) and anti-mouse IgG HRP (1/10 000 dilution) were purchased from Sigma-Aldrich. For immunoblotting, 50 μg of total protein was separated by SDS–PAGE, transferred onto nitrocellulose membrane (0.45 μm; Macherey-Nagel, Duren, Germany), and blocked for 45 min at room temperature with 5% non-fat milk dissolved in tris buffer saline supplemented with 0.05% tween-20 (TBST). After three washes with TBST, membranes were incubated overnight at 4 °C with primary Ab and for 1 h at room temperature with the appropriate secondary Ab followed by enhanced chemiluminescence (ECL) (Amersham Biosciences, Pittsburgh, PA).

Assessment of cell culture growth

To assay cell growth we used a cell counting technique. Cells were plated in 24-well plates and allowed to adhere overnight. The following day, cells were transduced with the corresponding adenoviruses as described above and incubated for further 48–96 h. Cells were then brought into suspension with 0.25% trypsin/EDTA, washed with growth medium supplemented with 10% FBS and re-suspended in 2% paraformaldehyde. The cells were counted in a hemocytometer. All samples were counted in triplicate. Mean values ± standard deviations were calculated for cell numbers determined by hemocytometer count. Unless otherwise stated, results are expressed as percentage growth of RAd-hCD40L transduced cultures relative to control virus-infected cells. (3-(4,5-Dimethylthiazol-2-yl)-25-diphenyltetrazoliam bromide) (MTT) conversion assays were also used to measure cell culture growth and drug-induced cytotoxicity as described earlier.[28]

Quantitative measurement of apoptosis

Apoptosis was measured by direct determination of nucleosomal DNA fragmentation using the 'Cell Death Detection Elisa Plus' kit (Roche Applied Science, Mannheim, Germany). Cells were plated in 96-well plates at an initial concentration $8–15 \times 10^3$ cells/well depending on the cell line. The following day, cells were infected with the corresponding adenoviruses as described above and treated with chemotherapeutics or left untreated. Alternatively, cells were exposed to rsCD40L (Alexis Corp., Enzo Life Sciences, Farmingdale, NY) or vehicle control and incubated for a further 24–48 h in the presence or absence of chemotherapy. Cells were then processed according to the manufacturer's protocol. The mono- and oligo-nucleosomes contained in the cell lysates were determined using the anti-histone–biotin Ab. The concentration of the mono- and oligo-nucleosomes was determined photometrically using an anti-histone–biotin Ab, followed by incubation with 2,2′-azino-di(3-ethylbenzthiazolin-sulfonate) (ABTS) as substrate for the antibody. The optical density (OD) was read on a Bio-Rad Microplate reader (Bio-Rad, Hercules, CA) at a wavelength of 405 nm. The data are expressed in photometric units and each unit corresponds to ~12 500 apoptotic cells. The data are presented as percentage of apoptotic cells on the basis of cell counts.

Xenograft model

Four million EJ tumor cells were injected subcutaneously into athymic nude mice. When tumors were approximately 20–30 mm^2, mice were treated three times (day 0, 3 and 6) with intratumoral injections of RAd-hCD40L (1×10^9 f.f.u.) or control virus. Tumor size was monitored 2–3 times a week using a caliper. Mice with tumors >100 mm^2 were killed. All animal experiments were approved by the local ethical committee in Uppsala, Sweden, Dnr: C260/7.

Statistical analysis

Statistical analysis was performed using Microsoft Analyseit by Excel or SigmaStat v.3.5 software. The methods of analyses were calculations of standard error of mean (s.e.m.), standard deviation (s.d.) and independent samples' *t*-test. As mouse survival or no survival is an ordinal and not a continuous scale, the results shown in Figure 7b were evaluated with Mann–Whitney *U*-test. Synergism (Figure 8) was concluded when $(\mu_{both}-\mu_{neither}) > (\mu_A-\mu_{neither})+(\mu_B-\mu_{neither})$, where $(\mu_{both}-\mu_{neither})$ is the response to both treatments A and B together and $(\mu_A-\mu_{neither})+(\mu_B-\mu_{neither})$ is the response to treatment A alone plus the response to treatment B alone, as described in Ref.[29].

Results

Adenovirus-mediated expression of human CD40L in vitro

We have generated a replication-deficient RAd vector in which expression of the human CD40L gene is driven by the cytomegalovirus promoter. This virus, RAd-hCD40L, was used to infect a panel of human carcinoma cell lines, namely the EJ, VM-CUB1 and T24 bladder, the CaSki and HeLa cervical and the AGE60 ovarian carcinoma line. Expression of CD40L was determined 24 h post infection by using immunofluorescence staining followed by flow cytometry. The results of this evaluation confirmed cell surface expression of CD40L in RAd-hCD40L-infected cells, which was proportional to the number of infectious particles used (Figure 1). Thus, at MOI 100, almost the entire population of each infected line expressed CD40L (Figure 1a). The mean fluorescence intensity of CD40L expression was higher in RAd-hCD40L-infected T24 and AGE60 compared with EJ, VM-CUB1, CaSki or HeLa cells, particularly, at MOI 50–100 (Figure 1b). Expression of CD40L was confirmed by immunoblot analysis of cell lysates from EJ cells infected with increasing MOI of RAd-hCD40L (Figure 1c). In contrast, no CD40L was detected after infection with RAd-lacZ, a control virus expressing β-galactosidase (Figure 1c).

Table 1 shows that with the exception of HeLa, all other carcinoma lines tested expressed CD40. To examine whether RAd-hCD40L infection results in CD40 stimulation, lysates from EJ cells infected with CD40L or β-galactosidase-expressing virus were analyzed for c-Jun N-terminal kinase (JNK) activation, a pathway known to be activated by soluble CD40L or agonistic CD40 mAb treatment of malignant cells.[10,30] As shown in Figure 1d, RAd-hCD40L induced sustained phosphorylation of JNK compared with rsCD40L protein that only transiently activated this pathway.

RAd-hCD40L inhibits the proliferation of CD40-positive tumor cell lines

The *in vitro* effects of RAd-hCD40L infection on carcinoma cell proliferation were evaluated. First, EJ cultures were infected with RAd-hCD40L or control lacZ-expressing virus at MOI 100 and changes in cell number were monitored over a period of 96 h. It was found that RAd-lacZ-infected cells displayed a time-dependent increase in proliferation similar to uninfected cultures, whereas infection with RAd-hCD40L resulted in significant growth retardation (Figure 2a). Thus, a 45% reduction in EJ cell number was observed at 48 h post infection with RAd-hCD40L relative to control virus. This further increased to approximately 55% at 72 h and

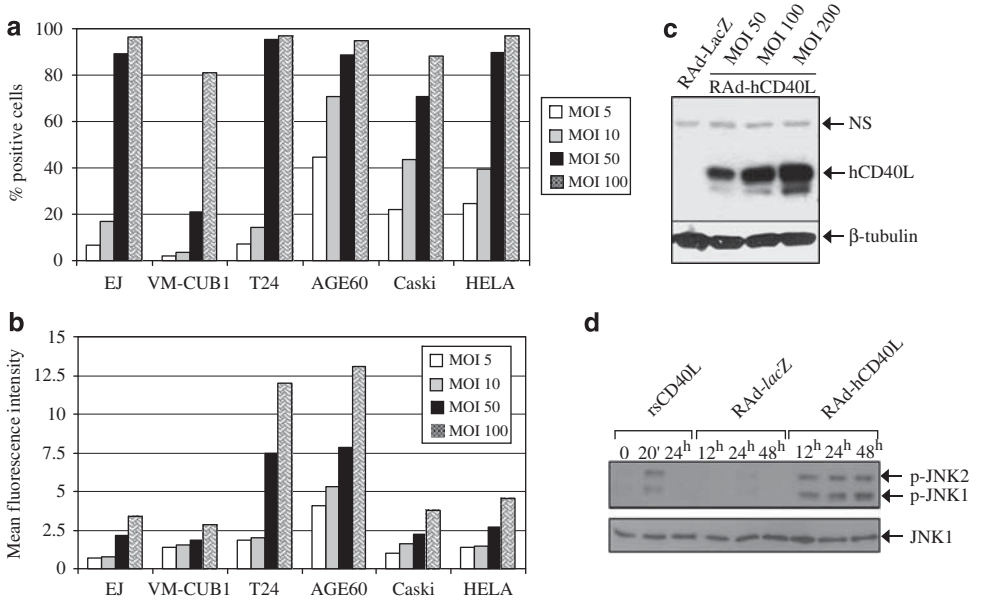

Figure 1 Expression of CD40L in RAd-hCD40L-infected tumor cell lines. (**a** and **b**) EJ, T24 and VM-CUB1 bladder carcinoma, CaSki and HeLa cervical and AGE60 ovarian carcinoma cells were infected with either RAd-hCD40L or RAd-lacZ at increasing multiplicity of infection (MOI). The percentage of cells expressing cell surface CD40L (**a**), and the mean fluorescence intensity (MFI) that is a measure of the levels of CD40L expressed (**b**) were determined by flow cytometry at 48 h post infection. Data represent mean values from two independent experiments. (**c**) Lysates from EJ cells infected with either increasing MOI of RAd-hCD40L or with RAd-lacZ at MOI 100 were immunoblotted with an anti-CD40L polyclonal antibody. Equal protein loading was confirmed by the presence of a non-specific (NS) band on the same gel or by re-probing the same membrane with an anti-β-tubulin antibody. (**d**) RAd-hCD40L induces constitutive engagement of JNK, a CD40-trigered signaling pathway. Lysates from EJ cells infected with RAd-hCD40L or RAd-lacZ at MOI 100 were collected at various time intervals and immunoblotted with an anti-phospho-JNK (Ser^{473}) polyclonal antibody. As a control,[10] cells were stimulated with 1 μg ml^{-1} recombinant soluble CD40L (rsCD40L) protein before analysis.

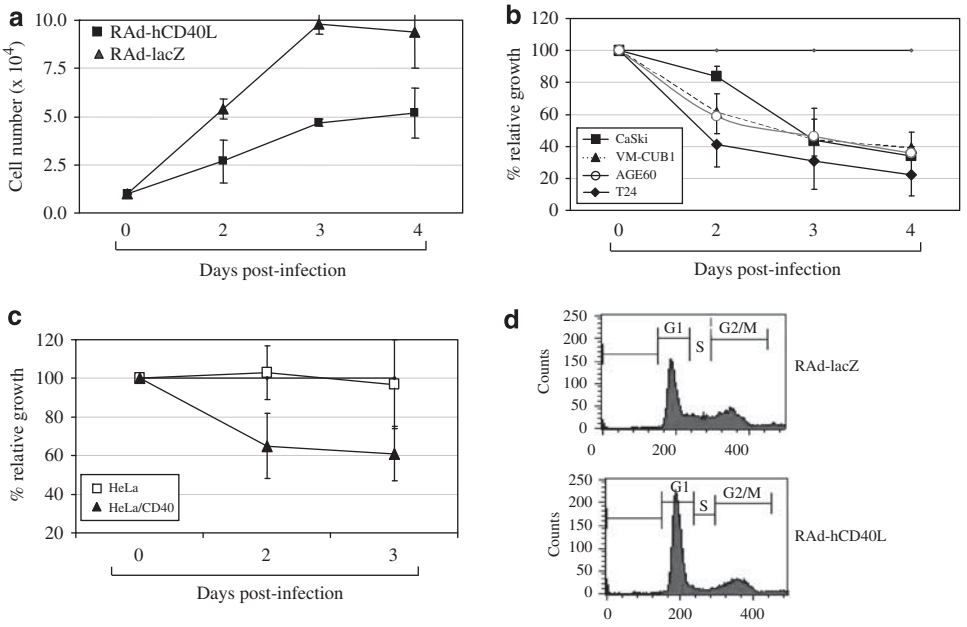

Figure 2 Inhibition of tumor cell proliferation by RAd-hCD40L. (**a**) EJ cells were transduced with RAd-hCD40L or control RAd-lacZ virus expressing β-galactosidase at MOI 100 and cell number was monitored on days 2, 3 and 4 post infection. Data are presented as the mean ± s.d. of three independent experiments each performed in triplicate. Differences in each time point were statistically significant as determined by the student's *t*-test ($P<0.01$). (**b**) T24 and VM-CUB1 bladder carcinoma, AGE60 ovarian and CaSki cervical carcinoma cells were transduced with RAd-hCD40L or RAd-lacZ as described in 'Materials and methods' and cell number was monitored for up to 4 days post infection. Data (mean values ± s.d. of three independent experiments) are depicted as the relative growth in RAd-hCD40L-infected cell cultures relative to control (RAd-*lac*Z infected), which were given the arbitrary value of 100%. Differences in each time point between RAd-hCD40L and control virus transduced cells were statistically significant as determined by the student's *t*-test ($P<0.01$). (**c**) HeLa and CD40-transfected HeLa cells (clone 14) were infected with RAds at MOI 10 and their proliferation rate was assessed at various time intervals. Results are depicted relative to the growth of RAd-lacZ-infected cultures, which were given the arbitrary value of 100%. Differences in each time point were statistically significant as determined by the student's *t*-test ($P<0.05$). (**d**) RAd-hCD40L induces accumulation of EJ cells to G0/G1 phase. EJ cells were transduced with RAd-hCD40L or RAd-lacZ virus at MOI 100 and 48 h later were fixed, stained with propidium iodide and their DNA content was analyzed by flow cytometry. Data are representative of two independent experiments.

was still significant at 96 h post infection (Figure 2a). The RAd-hCD40L-mediated suppression of proliferation was not particular to EJ cells as similar observations were made for T24, VM-CUB1, CaSki and AGE60 carcinoma cells (Figure 2b). However, no direct correlation between levels of CD40 expression and the extent of response to RAd-hCD40L was observed (see Table 1; Figure 2b).

To confirm that the RAd-hCD40L-mediated growth inhibition requires expression of CD40 in carcinomas, we stably transfected HeLa cells with a human CD40-expression vector. One of the derived clones, HeLa/CD40 clone 14, was found to express CD40 at levels comparable to other carcinoma cell lines under study (Table 1). This clone and parental HeLa cells were infected with RAd-lacZ or RAd-hCD40L and proliferation was assessed at various time intervals. Although the proliferation of CD40-negative HeLa cells remained unaffected by RAd-hCD40L, the CD40-expressing HeLa clone responded with growth inhibition (Figure 2c).

Cell-cycle analysis was performed in RAd-CD40L transduced EJ cell cultures using propidium iodide staining followed by flow cytometry. The results showed a dramatic decrease in the percentage of cells in S phase relative to RAd-lacZ-transduced cultures (5 vs 12.4%) and concomitant increased accumulation at the G0/G1 phase (66.5 vs 48.5%, respectively; Figure 2d).

Induction of cell death by RAd-hCD40L in human cancer cell lines

Treatment of carcinoma cells with rsCD40L protein in combination with protein synthesis inhibitors or antagonists of the PI3 kinase signaling pathway induces apoptosis.[16–18] We reasoned that the growth retardation observed in CD40-positive carcinoma lines infected with RAd-hCD40L (Figure 2) could result from induction of cell death. To test this hypothesis, we used a sensitive ELISA-based assay that detects mono- and oligo-nucleosomes in apoptotic cells (see 'Materials and methods'). Relative to control virus, RAd-hCD40L was found to induce EJ and VM-CUB1 cell killing at all MOI tested (Figures 3a and b, upper panels). This effect was abolished in the presence of a broad spectrum caspase inhibitor, zVAD.fmk (data not shown), further suggesting that the mode of cell death observed is apoptosis. To define the correlation between inhibition of growth and cell death, the effects of RAd-hCD40L on EJ and VM-CUB1 cell proliferation were assessed in parallel with apoptosis. The results showed that RAd-hCD40L induced

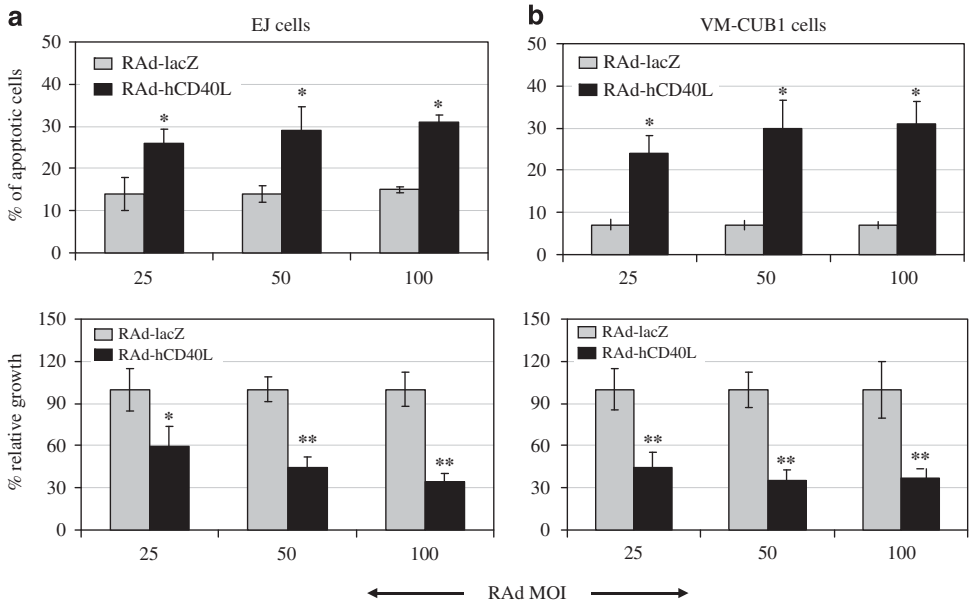

Figure 3 Induction of carcinoma cell death and growth inhibition after transduction with RAd-hCD40L. EJ (**a**) and VM-CUB1 (**b**) tumor cell lines were transduced with RAd-hCD40L or control virus (RAd-*lac*Z) at increasing MOI and apoptosis (upper panels) and relative cell growth (lower panels) were assessed 48 h post infection as described in 'Materials and methods'. Mean values (±s.d.) from three independent experiments (each performed in duplicate) for each cell line are shown. The difference between the groups (RAd-hCD40L vs RAd-*lac*Z) was statistically significant as determined by student's *t*-test (*$P<0.05$, **$P<0.01$).

a dramatic reduction in cell number, which was higher than the effect of this virus on cell death (Figure 3). Therefore, different or complementary mechanisms may operate to regulate RAd-hCD40L-induced apoptosis and growth inhibition, as documented earlier for soluble CD40L forms.[16]

The cytotoxic effect of RAd-hCD40L was confirmed in additional tumor cell lines such as the T24 bladder, CaSki cervical and AGE60 ovarian carcinoma (Figures 4a–c). Moreover, HeLa/CD40 clone 14 cells also responded to RAd-hCD40L with apoptosis induction whereas parental, CD40-negative HeLa cells remained unaffected (Figure 4d).

To determine whether 'fratricide' or 'suicide' is the dominant mechanism of apoptosis induction in CD40L-expressing cell cultures, HeLa cells, which are CD40-negative and therefore unresponsive to the cytotoxic effects of CD40L (Figure 4d), were transduced with either RAd-lacZ or RAd-hCD40L and then used as effectors in co-cultures with EJ cells. Significant EJ cell death was observed at effector:target ratio 2.5:1 (Figure 4e), suggesting that RAd-hCD40L transduced cells elicit strong bystander apoptotic effect.

Soluble CD40L does not modulate RAd-hCD40L-induced apoptosis in carcinoma cells

Members of the TNF family, such as Fas ligand (FasL), TRAIL and TNF, are found as both membrane-bound and soluble forms, the latter being generated on metalloproteinase-mediated cleavage of the membrane-tethered ligands. Soluble TRAIL is known to stimulate tumor cell death whereas locally produced soluble FasL antagonizes the pro-apoptotic effects of its membrane-bound form.[31–33]

In light of the cytotoxic properties of RAd-hCD40L in carcinomas (Figure 3), we asked whether soluble CD40L is generated by RAd-hCD40L transduced cells and influences their survival. Of note, the cleavage site of FasL[34] contains a sequence, which shares similarity with the extracellular domain of CD40L (Figure 5a) and soluble CD40L is produced by activated T lymphocytes through transmembrane cleavage of its membrane-bound form.[35] To this end, EJ cells were transduced with different MOI of RAd-hCD40L and culture supernatants were analyzed for the presence of soluble CD40L by ELISA. This analysis identified low but detectable levels of CD40L in these supernatants, which were proportional to the MOI used, reaching a maximum of approximately 12.5 ng ml^{-1} (±2.3) soluble CD40L in cells infected with RAd-hCD40L at MOI 100 (Figure 5b). To exclude the possibility that the soluble cytokine detected is released non-specifically by dying cells, we measured CD40L in the supernatants of RAd-hCD40L transduced EJ cultures treated with the broad spectrum caspase inhibitor zVAD-fmk. Under these conditions, zVAD-fmk abolished the apoptotic effects of RAd-hCD40L (data not shown) but did not influence the levels of soluble CD40L produced (Figure 5c). Moreover, HeLa cells that do not apoptose following transduction with RAd-hCD40L were found to produce significant concentrations of soluble CD40L (Figure 5c).

These observations prompted us to evaluate the effects that soluble CD40L might have on tumor cell survival. EJ carcinoma cells were cultured for 48 h with 7.5, 100 or

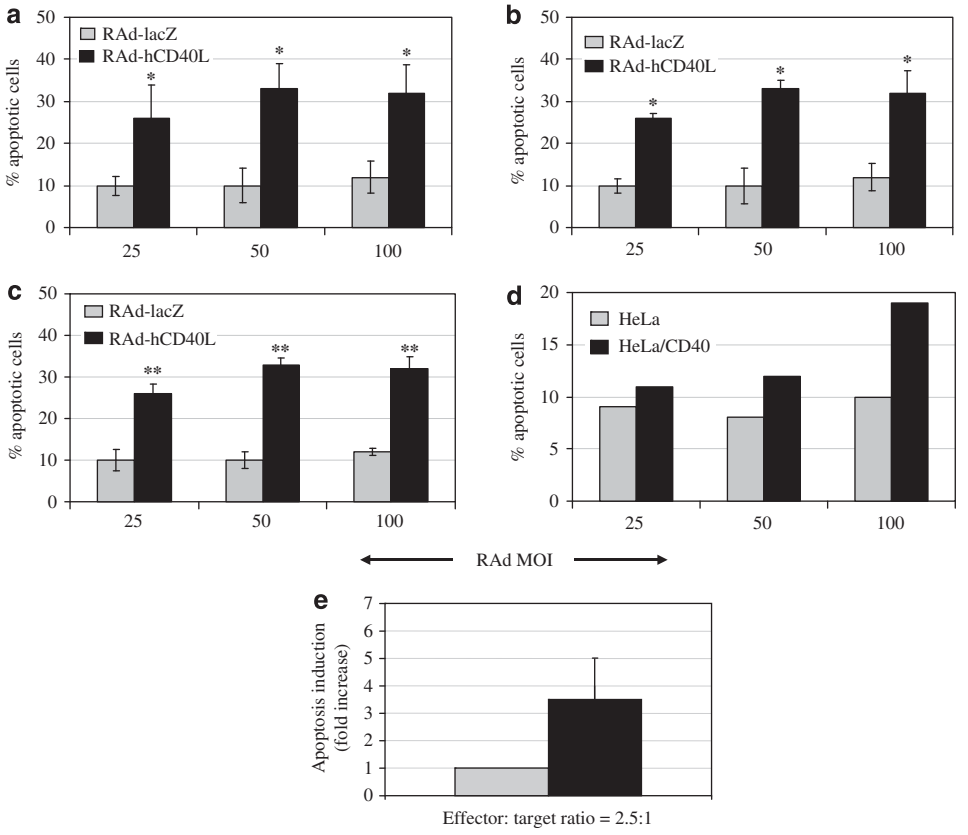

Figure 4 RAd-hCD40L induces apoptosis in carcinoma cell lines largely through a bystander effect. Apoptosis induced by RAd-hCD40L in T24 bladder (**a**), AGE60 ovarian (**b**) and CaSki cervical carcinoma cells (**c**) was measured by Cell Death ELISA and expressed as percentage apoptotic cells ± s.d. (*$P<0.05$, **$P<0.01$). (**d**) Specificity of RAd-hCD40L-induced apoptosis. HeLa/CD40 clone 14 and parental, CD40-negative HeLa cells were transduced with RAd-hCD40L at MOI 10 and 48 h later were analyzed for apoptosis induction using a Cell Death ELISA assay. The percentage of apoptotic cells (*y* axis) was calculated and depicted in histogram form relative to the MOI used (*x* axis). RAd-*lac*Z transduced HeLa/CD40 clone 14 or parental cells displayed only background (5–8%) levels of apoptosis (not shown). (**e**) CD40L expressed on the surface of RAd-hCD40L transduced cells induces bystander cytotoxicity. CD40-negative HeLa cells were transduced with RAd-lacZ or RAd-hCD40L at MOI 10 (effector cells) and 24 h later were mixed with non-transduced EJ cells (targets) at a ratio of 2.5:1. EJ carcinoma cell death was measured 48 h later by Cell Death ELISA. Data show the fold increase in apoptosis induced by RAd-hCD40L (Black bar) relative to RAd-*lac*Z (Grey bar), which was given the arbitrary value of 1. Mean values ± s.d. from three independent measurements are shown.

$1000\,ng\,ml^{-1}$ rsCD40L protein and apoptosis was assessed using a Cell Death ELISA assay. It was found that exposure to rsCD40L concentrations up to $100\,ng\,ml^{-1}$ did not elevate apoptosis above background levels whereas a small increase in the percentage of apoptotic cells was observed at the high dose of $1000\,ng\,ml^{-1}$ rsCD40L (Figure 5d). Therefore, soluble CD40L does not induce carcinoma cell death at concentrations similar to those detected in RAd-hCD40L-transduced cultures.

As soluble FasL has been shown earlier to antagonize RAd-FasL-induced cytotoxicity[36] we questioned whether soluble CD40L may likewise interfere with the pro-apoptotic properties of RAd-hCD40L in carcinoma cells. Thus, EJ cells were infected with RAd-hCD40L or RAd-lacZ at MOI 100 and then exposed to increasing concentrations of rsCD40L before assessment of apoptosis by a sensitive Cell Death ELISA. As shown in Figure 5e, the effect of RAd-hCD40L on apoptosis remained unaffected by the presence of soluble CD40L. We conclude that CD40L is released by RAd-hCD40L transduced carcinoma cells but that soluble CD40L does not modulate the apoptotic cell response to its membrane-bound form.

Apoptotic effects of a C194W-mutated CD40L-expressing adenovirus

An earlier report has shown that a cysteine 194 to tryptophane ($C^{194}\rightarrow W$) mutation in the extracellular domain of CD40L enhances the *in vitro* binding capacity of soluble CD40L to its receptor.[37] This observation raised the possibility that an adenovirus vector expressing the C194W-mutated CD40L (RAd-hmutCD40L) could confer more potent pro-apoptotic effects than its wild-type equivalent. We therefore used site-directed mutagenesis to generate a $C^{194}\rightarrow W$ expressing CD40L construct and cloned the mutated product into an adenovirus vector under the control of the cytomegalovirus promoter. Recombinant virus was produced and used to infect EJ cells in parallel with RAd-hCD40L. Expression of mutated CD40L was similar to the wild-type equivalent

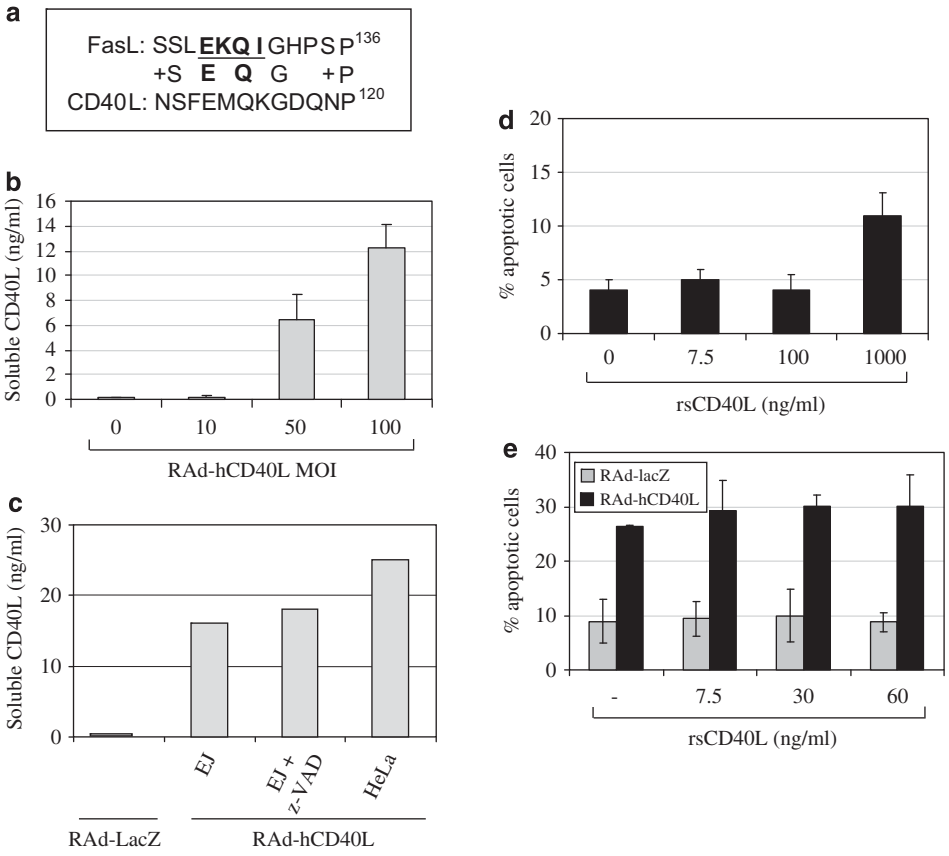

Figure 5 Soluble CD40L does not modulate RAd-hCD40L-induced apoptosis in carcinoma cells. (**a**) Amino acid alignment of FasL and CD40L identifies a region in the extracellular domain of CD40L that shows similarity with the cleavage site of FasL, *EKQI* (bold characters) (Ref.[32]). (**b**) Soluble CD40L is detected in the supernatants of tumor cells infected with RAd-hCD40L. EJ bladder carcinoma cells were transduced with RAd-hCD40L at MOI 10, 50 or 100 and culture supernatants were analyzed 48 h later for the presence of soluble CD40L by ELISA; values are presented as the mean ± s.d. of three independent experiments. (**c**) Soluble CD40L is not produced non-specifically by dying RAd-hCD40L transduced cells. EJ cells were transduced with RAd-hCD40L or RAd-*lac*Z and then incubated with 40 μM of the caspase inhibitor zVAD-fmk before evaluation of apoptosis and of CD40L levels in culture supernatants. zVAD-fmk completely suppressed EJ cell death (not shown). Additionally, soluble CD40L was evaluated by ELISA in supernatants of HeLa cell cultures transduced with RAd-hCD40L or RAd-*lac*Z at MOI 10. (**d**) Soluble CD40L does not induce carcinoma cell death at concentrations similar to those detected in RAd-hCD40L transduced cultures. EJ cells were treated for 48 h with increasing concentrations of recombinant soluble CD40L (rsCD40L), as indicated, before assessment of apoptosis by Cell Death ELISA; values are presented as the mean ± s.d. of four independent experiments. (**e**) Soluble CD40L does not influence RAd-hCD40L-induced apoptosis. EJ carcinoma cells were transduced with RAd-hCD40L or RAd-lacZ at MOI 100 and 8 h later rsCD40L protein was added at increasing concentrations, as indicated. Apoptosis was assessed 48 h later by a Cell Death ELISA as described in 'Materials and methods'.

as determined by flow cytometry in RAd-infected EJ cells (not shown). Apoptosis was assessed 48 h post infection and compared with the effect of wild-type CD40L-expressing adenovirus. The results showed that the C194W mutation did not increase the cytotoxic activity of RAd-hCD40L (Figure 6).

In vivo *anti-tumor activity of RAd-hCD40L*

On the basis of the aforementioned observations, we focused on RAd expressing wild-type hCD40L and evaluated its *in vivo* anti-tumor activity. Athymic nude mice were injected subcutaneously with EJ human tumor cells. Once tumors reached approximately 20–30 mm^2 in size, mice were treated a total of three times (days 0, 3 and 6) with intratumoral injections of RAd-hCD40L or control virus. Mice were monitored for tumor growth and survival and killed when the tumor size reached 100 mm^2 (end point). By day 30 after initiation of treatment, all control virus-administered mice had reached end point. In contrast, the growth of RAd-hCD40L-treated tumors was significantly retarded such that three out of five of the tumor-bearing mice survived at least up to day 40 (Figures 7a and b). At this point, one of the remaining three RAd-hCD40L-treated mice showed complete remission, one had a stable disease (9 mm^2) and the third mouse had a slowly progressing tumor (55 mm^2).

Immunohistochemical evaluation of active caspase-3 in tumors resected from euthanized mice showed significantly more apoptotic cells in RAd-hCD40L than control virus-treated tumors (Figures 7c–e). Although the number of caspase-3-positive cells appears to be low, apoptosis is

a dynamic process in which dead or dying cells are rapidly removed by phagocytosis. It is therefore likely that the actual extent of tumor cell death in RAd-hCD40L-treated mice is higher than that detected by our analysis.

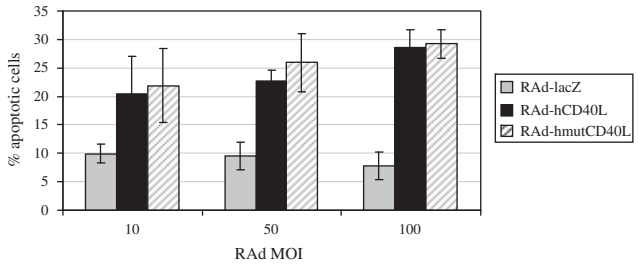

Figure 6 A RAd expressing C194W CD40L induces similar levels of cancer cell death as the wt CD40L virus. EJ cells were infected with RAd-hCD40L, RAd-hmutCD40L-expressing C194W CD40L or control virus (RAd-*lac*Z) at MOI 100 and apoptosis was assessed 48 h post infection using a Cell Death ELISA assay as described in 'Materials and methods'. The percentage of apoptotic cells (*y* axis) was calculated and depicted in histogram form relative to the MOI used (*x* axis). Mean values from three independent experiments for each cell line are shown.

RAd-hCD40L synergizes with chemotherapy in inducing tumor cell killing

Tumor necrosis factor family members, such as TRAIL, have been shown to sensitize tumor cells to chemotherapy-induced apoptosis (reviewed in Ref.[38]). Our earlier work has showed that rsCD40L synergizes with certain anti-cancer drugs to induce cell death in CD40-transfected HeLa cells.[10] On the basis of this finding, we have investigated the hypothesis that RAd-hCD40L may also function in concert with chemotherapy to augment apoptosis in carcinoma cells. We have therefore analyzed the *in vitro* cytotoxic effects of RAd-hCD40L in combination with the DNA damaging agents *cis*-platin and mitomycin C and of the anti-metabolite 5-fluorouracil (5FU), all of which are widely used for the treatment of various types of human cancer. Thus, EJ bladder carcinoma cells were infected with RAd-hCD40L or RAd-*lac*Z at MOI 100 and then treated with 10 μM *cis*-platin, 500 μM 5FU or 2 μg ml^{-1} mitomycin C before assessment of apoptosis. As shown in Figure 8a, the drug concentrations used had a relatively small impact on the viability of RAd-*lac*Z-infected cells, inducing 15–40% apoptosis. In marked contrast, however, the combination of chemotherapy and RAd-hCD40L significantly enhanced tumor cell killing by 2- to 7-fold (Figure 8a). We

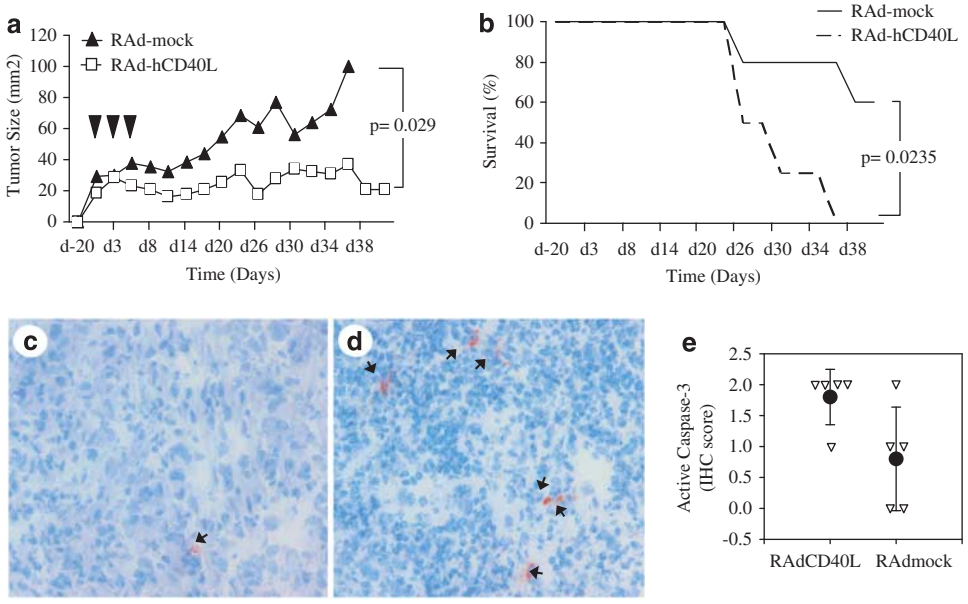

Figure 7 RAd-CD40L inhibits tumor growth *in vivo*. Athymic nude mice were xenotransplanted with 4×10^6 EJ cells. When 20–30 mm^2 tumors were formed (day 20), mice were injected intratumorally with 1×10^9 f.f.u. RAd-hCD40L ($n = 5$) or control virus ($n = 5$) (solid arrowhead). Viruses were also administered on days 3 and 6 and tumor volumes (**a**) and animal survival (**b**) were determined as described in 'Materials and methods'. The tumor volumes and survival in the RAd-Mock and RAd-hCD40L-treated animals differed significantly at day 40 as determined by independent samples' *t*-test ($\alpha = 0.05$; $P = 0.0290$) and Mann–Whitney *U*-test ($\alpha = 0.05$, $P = 0.0235$), respectively. The experiment was repeated twice with similar results; (**c** and **d**) show immunohistochemical analysis of active caspase-3 in tumor sections from RAd-Mock and RAd-hCD40L-treated mice, respectively. Active caspase-3 expression was investigated using rabbit anti-human/mouse active caspase-3 (R&D Systems, Abingdon, UK). Primary antibody was allowed to incubate for 30 min at RT, followed by Rabbit EnVision System Labeled Polymer-HRP and AEC Substrate Chromogen (DAKO, Glostrup, Denmark). Tissue sections were counterstained with hematoxylin and mounted before analyzed using Leica DFC280 at 10×40 magnifications. Positive cells are shown by arrows. The staining was scored as follows: negative sections = 0, occasional cells in the section = 1 (as in **c**) and scattered cells in the section = 2 (as in **d**). The results are summarized in histogram form (**e**) in which individual scores are shown by arrowheads. The difference between the groups were determined by independent samples' *t*-test ($\alpha = 0.05$, $P = 0.0462$).

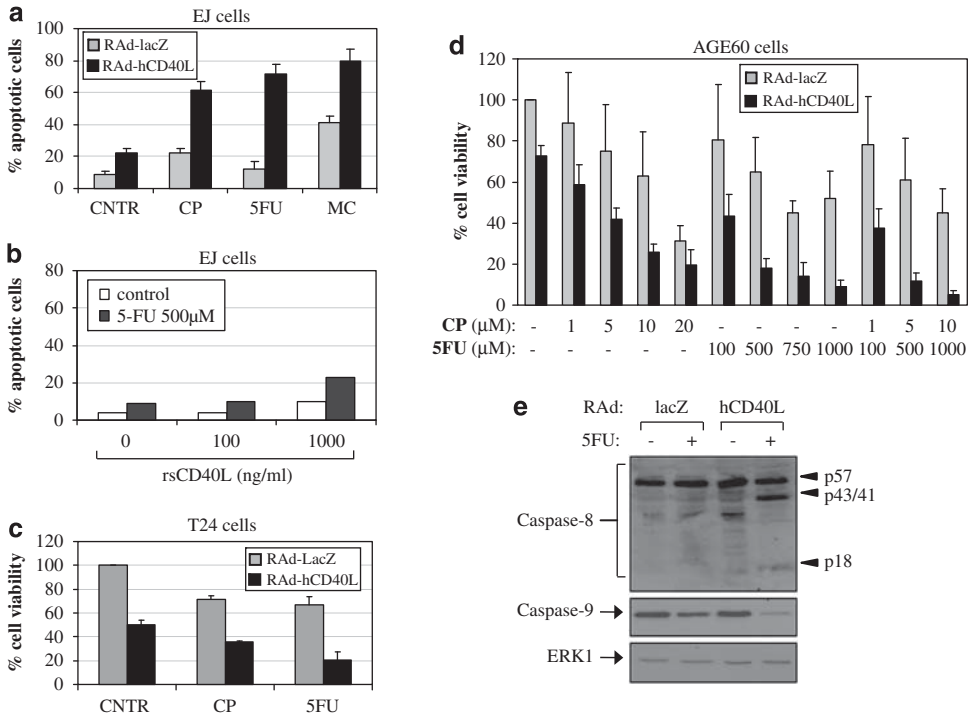

Figure 8 RAd-CD40L and chemotherapy synergize to induce tumor cell death. (**a**) RAd-hCD40L synergizes with chemotherapy to amplify EJ bladder carcinoma cell killing. EJ cells were transduced with RAd-hCD40L or RAd-lacZ at MOI 50 and 8 h post infection were exposed to 10 μM *cis*-platin (CP) or 500 μM 5FU for an additional 40 h period. Apoptosis was assessed by a Cell Death ELISA; values are presented as the mean percentage apoptotic cells ± s.d. of three independent experiments. Synergism was concluded on the basis of the statistical analysis described in 'Materials and methods'. (**b**) High concentrations of recombinant soluble CD40L (rsCD40L) in combination with 5FU marginally increase EJ tumor cell death. EJ cells were treated with rsCD40L at 0, 100 or 1000 ng ml^{-1} in the presence or absence of 500 μM 5FU and apoptosis was evaluated 48 h later. (**c**) RAd-hCD40L synergizes with chemotherapy to amplify T24 bladder carcinoma cell killing. T24 cells were treated as described in (**a**) and cytotoxicity was determined by MTT conversion assays. Data shown as % viability relative to control RAd-lacZ-infected cultures that were given the arbitrary value of 100. Values are presented as the mean percentage viability ± s.d. of three independent experiments. (**d**) RAd-hCD40L enhances the cytotoxic effects of chemotherapy in AGE60 ovarian carcinoma cells. AGE60 cells were transduced with RAd-hCD40L or RAd-lacZ at MOI 25 and 8 h post infection were exposed to increasing concentrations of CP or 5FU for an additional 40 h period. Cell survival was assessed by MTT conversion assays. Data are shown as % viability relative to control RAd-lacZ-infected cultures that were given the arbitrary value of 100. Values are presented as the mean ± s.d. of three independent experiments, each performed in triplicate determinations. (**e**) RAd-hCD40L and 5FU combination treatment induces caspase activation. EJ cells were treated as described in (**a**) and 30 h post infection cell lysates were analyzed for expression of caspase-8, caspase-9 or ERK1 by immunoblot. The cleaved products of caspase-8 (p57, p43/41 and p18) are indicated by arrowheads.

performed similar experiments using rsCD40L instead of RAd-hCD40L, as the former has been used recently in phase I clinical trials.[24] As shown in Figure 8b, high concentrations of rsCD40L (1000 ng ml^{-1}) were found to increase 5FU killing in EJ cells. However, the extent of apoptosis was low compared with the dramatic synergistic effect observed after 5FU and RAd-hCD40L combination treatment.

The cytotoxic effects of RAd-hCD40L and chemotherapy were also evaluated in T24 bladder and AGE60 ovarian carcinoma cells. T24 cultures were infected with RAd-hCD40L or RAd-lacZ at MOI 50 and then treated with either 10 μM *cis*-platin or 500 μM 5FU. Cell viability was assessed at 48 h by using the MTT conversion assay. The results confirmed that combinations of RAd-hCD40L with either *cis*-platin or 5FU are more effective in inducing carcinoma cell killing than each agent alone (Figure 8c).

A more detailed analysis of combination therapy treatments was performed in AGE60 cells. After infection with RAd-hCD40L or RAd-lacZ at MOI 10, AGE60 cells were exposed to increasing concentrations of *cis*-platin (1–20 μM), 5FU (100–1000 μM) or both drugs and viability were assessed 48 h later by MTT conversion assays. In RAd-*lac*Z-transduced cells, 5FU caused a concentration-dependent decrease in viability, which reached a maximum of 50% at 750–1000 μM drug concentrations (Figure 8d). However, cytotoxicity was dramatically enhanced when RAd-hCD40L was used instead of RAd-*lac*Z, resulting in more than 90% reduction in AGE60 cell viability at the highest 5FU concentration of 1000 μM. Similar potentiation of cell death was observed after RAd-hCD40L and *cis*-platin combination treatment, although cytotoxicity appeared to be additive rather than synergistic in this case (Figure 8d). Moreover, exposure of RAd-hCD40L-transduced AGE60 cells to

both 5FU and *cis*-platin resulted in further reduction in tumor cell viability (Figure 8d).

Caspase cleavage was evaluated in EJ cells transduced with RAd-hCD40L or RAd-*lac*Z at MOI 100 and then exposed to 500 μM 5FU for 30 h. The results showed reduction in pro-caspase-8 and significant accumulation of cleaved p18 and p43/41 caspase-8 in RAd-hCD40L transduced cells treated with 5FU compared with equivalent cultures transduced with control virus (Figure 8e). Likewise, the combination of RAd-hCD40L and 5FU induced dramatic reduction in the levels of pro-caspase-9, which is involved in the mitochondria-mediated death cascade, but not of the unrelated ERK1 kinase (Figure 8e). These data suggest that RAd-hCD40L synergizes with chemotherapy in inducing caspase activation and tumor cell killing.

Discussion

The central role of CD40 in orchestrating both the humoral and cell-mediated immune response is consistent with the major contribution of this pathway to the development of anti-tumor immunity. Indeed, mutations in the CD40L gene in human beings result in a rare immune disorder called the X-linked hyper IgM syndrome, which is characterized by impaired lymphoid cell function and increased susceptibility to malignancy.[39,40] Preclinical studies in syngeneic mouse tumor models have showed that CD40L administration activates the normal host antigen-presenting cell function, which enables anti-tumor responses.[41] Some of these studies have used a RAd to deliver murine CD40L either directly to tumors or to DCs in syngeneic models of colorectal, bladder, lung, prostate carcinoma or melanoma. CD40L delivery was found to stimulate the maturation of DCs in the tumor microenvironment, to counteract immune escape mechanisms and to elicit both tumor regression and protective anti-tumor immunity.[3–5,27,42]

The aforementioned assessments of the immunostimulatory effects of CD40L administration have been mostly performed in CD40-negative mouse tumor cell models. However, the majority of primary human carcinomas and established cancer cell lines express CD40 (reviewed in Ref.[21,22]), suggesting that further analyses are required to explore fully the therapeutic benefit of CD40L-based modalities. Indeed, the stimulation of human carcinoma cell lines with soluble CD40L or agonistic anti-CD40 mAbs has been reported to retard their proliferation.[12–15] CD40L also directly enhances the immunogenicity of CD40-positive malignant cells, resulting in their *in vitro* recognition and killing by antigen-specific $CD8^+$ cytotoxic T lymphocytes.[10,43] Importantly, normal epithelium is CD40-negative or expresses low levels of the receptor.[10] Together, these findings have set the stage for an early phase I clinical trial of systemic administration of rsCD40L, which confirmed that CD40 therapies are well tolerated, show minimal side effects and associate with anti-tumor activity.[24] The therapeutic potential of soluble CD40L is, however, hindered by its high *in vivo* turnover rate and poor pharmacokinetics.[24]

In this study, we have evaluated the concept that prolonged engagement of the CD40 pathway in malignant cells infected with a CD40L-expressing RAd (RAd-hCD40L) may confer potent anti-tumor effects. Replication-defective adenoviruses used in our study are among the most efficient vectors for transduction of eukaryotic cells. Indeed, high efficiencies of gene transfer were obtained using an MOI of 50 f.f.u. of RAd-hCD40L in all established carcinoma cell lines tested, achieving significant CD40L cell surface expression. The early passage ovarian carcinoma cell line AGE60, generated in our laboratory from the ascitic fluid of a woman with ovarian cancer, was efficiently transduced by RAd-hCD40L using as little as 5 f.f.u. of virus preparation (Figure 1). The RAd-mediated expression of CD40L in CD40-positive bladder, cervical and ovarian carcinoma cells significantly reduced their proliferation with concomitant accumulation at the G0/G1 phase of cell cycle (Figure 2). Importantly, RAd-hCD40L also reduced tumor growth *in vivo* and increased the survival of mice xenotransplanted with CD40-positive human carcinoma cells (Figure 7).

Our recently published work has showed that rsCD40L can deliver apoptotic signals to carcinoma cells, which are manifested only upon disruption of CD40-activated survival pathways, such as PI3 kinase/mTOR and ERK.[44] Data shown in this study reveal an unprecedented apoptotic function of RAd-hCD40L in carcinoma cells even in the absence of PI3 kinase or ERK inhibition. Thus, although high concentrations of soluble CD40L only marginally stimulate EJ cell death (Figure 5d), RAd-hCD40L induced apoptosis in approximately 20–30% of the infected cultures (Figure 3a). It is noteworthy that under the experimental conditions used, soluble CD40L and RAd-hCD40L induced similar levels of JNK activation (Figure 1d). This observation indicates that these treatments could achieve similar levels of receptor stimulation. The pro-apoptotic effect of RAd-hCD40L was specific for CD40 as infection with a control, β-galactosidase-expressing RAd did not influence EJ cell viability at a range of MOI and RAd-hCD40L had no effect on CD40-negative carcinoma cells (Figures 3a and 4d).

The observed difference between soluble and RAd-delivered CD40L in inducing apoptosis may reflect the oligomeric status of soluble vs membrane-tethered CD40L. Earlier studies have shown that the extent of CD40L oligomerization influences CD40 signaling[45] and apoptosis induction in susceptible carcinoma cell lines.[16] Presumably, the CD40-binding capacity of membrane-tethered CD40L suffices for optimal receptor stimulation and apoptosis induction and is thus not influenced by the $C^{194} \rightarrow W$ modification (Figure 6), which enhances the stimulatory capacity of soluble CD40L.[37] It is also possible that the elevated levels of RAd-hCD40L-induced apoptosis are the result of the constitutive stimulation of CD40 by CD40L expressed in infected cells. Concomitant with this idea, RAd-hCD40L but not soluble CD40L displays prolonged engagement of the JNK signaling

pathway (Figure 1d), which has been implicated in the pro-apoptotic effects of CD40 ligation.[30]

The death-inducing and inflammatory activity of membrane-tethered FasL, a well-studied TNF family member, is regulated by soluble FasL, which is shed from the membrane-bound form of the molecule by putative metalloproteinase(s).[32,33] RAd-FasL-infected cells secrete soluble FasL that reduces the cytotoxic effects and therapeutic capacity of this virus.[36] We have found that unlike FasL, soluble CD40L does not antagonize the apoptotic effects of RAd-hCD40L on carcinoma cells (Figure 5). This observation serves to further highlight the advantages of using CD40L gene delivery for cancer therapy compared with other members of the TNF family.

Data shown in this study demonstrate that RAd-hCD40L is also superior to soluble CD40L in amplifying tumor cell killing in combination with chemotherapeutic agents. This is particularly evident in the context of 5FU and RAd-hCD40L combination treatment in bladder and ovarian carcinoma cells, which induces a synergistic *in vitro* cytotoxic effect at clinically relevant drug concentrations (Figure 8). Importantly, similar to CD40L,[10] 5FU sensitizes melanoma and carcinoma cells to antigen-specific cytotoxic T lymphocyte lysis[46,47] and the anti-tumor effects of chemotherapy have recently been shown to involve immune components.[48] It is therefore conceivable that far from reducing the immuno-modulatory properties of CD40 ligation, 5FU may operate at multiple levels to amplify tumor cell killing in combination with RAd-hCD40L, a concept that is currently under investigation.

Overall, the data shown in this report highlight the potential of exploiting the direct effects of CD40 ligation on human carcinomas using CD40L gene transfer alone or in combination with other modalities for cancer therapy. Our results have also broader implications in appreciating the multifaceted anti-tumor activities of the CD40 pathway in carcinomas thus paving the way for its future clinical application.

Conflict of interest

The authors declare no conflict of interest.

Acknowledgements

This work was supported by the European Commission FP6 program *Apotherapy* (EC contract number 037344; http://apotherapy.med.uoc.gr) to AGE and AL, an Association for Cancer Research (AICR, UK) grant to AGE and a kind donation from Mr N Tzimas (Athens, Greece).

References

1 Noelle RJ. CD40 and its ligand in host defense. *Immunity* 1996; **4**: 415–419.
2 van Kooten C, Banchereau J. CD40-CD40 ligand. *J Leukoc Biol* 2000; **67**: 2–17.
3 Mackey MF, Gunn JR, Maliszewski C, Kikutani H, Noelle RJ, Barth RJ. Dendritic cells require maturation via CD40 to generate protective anti-tumour immunity. *J Immunol* 1998; **161**: 2094–2098.
4 Kikuchi T, Crystal RG. Anti-tumor immunity induced by *in vivo* adenovirus vector-mediated expression of CD40 ligand in tumor cells. *Hum Gene Ther* 1999; **10**: 1375–1387.
5 Sun Y, Peng D, Lecanda J, Schmitz V, Barajas M, Qian C *et al*. *In vivo* gene transfer of CD40 ligand into colon cancer cells induces local production of cytokines and chemokines, tumor eradication and protective antitumor immunity. *Gene Ther* 2000; **7**: 1467–1476.
6 Loskog A, Dzojic H, Vikman S, Ninalga C, Essand M, Korsgren O *et al*. Adenovirus CD40 ligand gene therapy counteracts immune escape mechanisms in the tumor microenvironment. *J Immunol* 2004; **172**: 7200–7205.
7 Noguchi M, Imaizumi K, Kawabe T, Wakayama H, Horio Y, Sekido Y *et al*. Induction of antitumor immunity by transduction of CD40 ligand gene and interferon-gamma gene into lung cancer. *Cancer Gene Ther* 2001; **8**: 421–429.
8 Loskog A, Bjorkland A, Brown MP, Korsgren O, Malmstrom PU, Totterman TH. Potent antitumor effects of CD154 transduced tumor cells in experimental bladder cancer. *J Urol* 2001; **166**: 1093–1097.
9 Loskog AS, Fransson ME, Totterman TT. AdCD40L gene therapy counteracts T regulatory cells and cures aggressive tumors in an orthotopic bladder cancer model. *Clin Cancer Res* 2005; **11**: 8816–8821.
10 Hill SC, Youde SJ, Man S, Teale GR, Baxendale AJ, Hislop A *et al*. Activation of CD40 in cervical carcinoma cells facilitates CTL responses and augments chemotherapy-induced apoptosis. *J Immunol* 2005; **174**: 41–50.
11 Sabel MS, Yamada M, Kawaguchi Y, Chen FA, Takita H, Bankert RB. CD40 expression on human lung cancer correlates with metastatic spread. *Cancer Immunol Immunother* 2000; **49**: 101–108.
12 Eliopoulos AG, Dawson CW, Mosialos G, Floettmann JE, Rowe M, Armitage RJ *et al*. CD40-induced growth inhibition in epithelial cells is mimicked by Epstein-Barr virus-encoded LMP1: involvement of TRAF3 as a common mediator. *Oncogene* 1996; **13**: 2243–2254.
13 Tong AW, Papayoti MH, Netto G, Armstrong DT, Ordonez G, Lawson JM *et al*. Growth-inhibitory effects of CD40 ligand (CD154) and its endogenous expression in human breast cancer. *Clin Cancer Res* 2001; **7**: 691–703.
14 Ghamande S, Hylander BL, Oflazoglu E, Lele S, Fanslow W, Repasky EA. Recombinant CD40 ligand therapy has significant antitumor effects on CD40-positive ovarian tumor xenografts grown in SCID mice and demonstrates an augmented effect with cisplatin. *Cancer Res* 2001; **61**: 7556–7562.
15 Hirano A, Longo DL, Taub DD, Ferris DK, Young LS, Eliopoulos AG *et al*. Inhibition of human breast carcinoma growth by a soluble recombinant human CD40 ligand. *Blood* 1999; **93**: 2999–3007.
16 Eliopoulos AG, Davies C, Knox PG, Gallagher NJ, Afford SC, Adams DH *et al*. CD40 induces apoptosis in carcinoma cells through activation of cytotoxic ligands of the tumor necrosis factor superfamily. *Mol Cell Biol* 2000; **20**: 5503–5515.
17 Grell M, Zimmermann G, Gottfried E, Chen CM, Grünwald U, Huang DC *et al*. Induction of cell death by tumour necrosis factor (TNF) receptor 2, CD40 and CD30: a role for TNF-R1 activation by endogenous membrane-anchored TNF. *EMBO J* 1999; **18**: 3034–3043.

18 Hess S, Engelmann H. A novel function of CD40: induction of cell death in transformed cells. *J Exp Med* 1996; **183**: 159–167.
19 Shaw NJ, Georgopoulos NT, Southgate J, Trejdosiewicz LK. Effects of loss of p53 and p16 function on life span and survival of human urothelial cells. *Int J Cancer* 2005; **116**: 634–639.
20 Davies CC, Bem D, Young LS, Eliopoulos AG. NF-kappaB overrides the apoptotic program of TNF receptor 1 but not CD40 in carcinoma cells. *Cell Signal* 2005; **17**: 729–738.
21 Eliopoulos AG, Young LS. The role of the CD40 pathway in the pathogenesis and treatment of cancer. *Curr Opin Pharmacol* 2004; **4**: 360–367.
22 Tong AW, Stone MJ. Prospects for CD40-directed experimental therapy of human cancer. *Cancer Gene Ther* 2003; **10**: 1–13.
23 Dallman C, Johnson PW, Packham G. Differential regulation of cell survival by CD40. *Apoptosis* 2003; **8**: 45–53.
24 Vonderheide RH, Dutcher JP, Anderson JE, Eckhardt SG, Stephans KF, Razvillas B *et al*. Phase I study of recombinant human CD40 ligand in cancer patients. *J Clin Oncol* 2001; **19**: 3280–3287.
25 O'Toole CM, Povey S, Hepburn P, Franks LM. Identity of some human bladder cancer cell lines. *Nature* 1983; **301**: 429–430.
26 Marshall CJ, Franks LM, Carbonell AW. Markers of neoplastic transformation in epithelial cell lines derived from human carcinomas. *J Natl Cancer Inst* 1977; **58**: 1743–1751.
27 Dzojic H, Loskog A, Totterman TH, Essand M. Adenovirus-mediated CD40 ligand therapy induces tumor cell apoptosis and systemic immunity in the TRAMP-C2 mouse prostate cancer model. *Prostate* 2006; **66**: 831–838.
28 Eliopoulos AG, Kerr DJ, Herod J, Hodgkins L, Krajewski S, Reed JC *et al*. The control of apoptosis and drug resistance in ovarian cancer: influence of p53 and bcl-2. *Oncogene* 1995; **11**: 1217–1228.
29 Slinker BK. The statistics of synergism. *J Mol Cell Cardiol* 1998; **30**: 723–731.
30 Georgopoulos NT, Steele LP, Thomson MJ, Selby PJ, Southgate J, Trejdosiewicz LK. A novel mechanism of CD40-induced apoptosis of carcinoma cells involving TRAF3 and JNK/AP-1 activation. *Cell Death Differ* 2006; **13**: 1789–1801.
31 Kim CY, Jeong M, Mushiake H, Kim BM, Kim WB, Ko JP *et al*. Cancer gene therapy using a novel secretable trimeric TRAIL. *Gene Ther* 2006; **13**: 330–338.
32 Suda T, Hashimoto H, Tanaka M, Ochi T, Nagata S. Membrane Fas ligand kills human peripheral blood T lymphocytes, and soluble Fas ligand blocks the killing. *J Exp Med* 1997; **186**: 2045–2050.
33 Schneider P, Holler N, Bodmer J-L, Hahne M, Frei K, Fontana A *et al*. Conversion of membrane-bound Fas (CD95) ligand to its soluble form is associated with downregulation of its proapoptotic activity and loss of liver toxicity. *J Exp Med* 1998; **187**: 1205–1213.
34 Tanaka M, Itai T, Adachi M, Nagata S. Downregulation of Fas ligand by shedding. *Nature Med* 1998; **4**: 31–36.
35 Matthies KM, Newman JL, Hodzic A, Wingett DG. Differential regulation of soluble and membrane CD40L proteins in T cells. *Cell Immunol* 2006; **241**: 47–58.
36 Knox PG, Milner AE, Green NK, Eliopoulos AG, Young LS. Inhibition of metalloproteinase cleavage enhances the cytotoxicity of fas ligand. *J Immunol* 2003; **170**: 677–685.
37 Matsuura JE, Morris AE, Ketchem RR, Braswell EH, Klinke R, Gombotz WR *et al*. Biophysical characterization of a soluble CD40 ligand (CD154) coiled-coil trimer: evidence of a reversible acid-denatured molten globule. *Arch Biochem Biophys* 2001; **392**: 208–218.
38 Lee JY, Huerta-Yepez S, Vega M, Baritaki S, Spandidos DA, Bonavida B. The NO TRAIL to YES TRAIL in cancer therapy (review). *Int J Oncol* 2007; **31**: 685–691.
39 Callard RE, Armitage RJ, Fanslow WC, Spriggs MK. CD40 ligand and its role in X-linked hyper-IgM syndrome. *Immunol Today* 1993; **14**: 559–564.
40 Hayward AR, Levy J, Facchetti F, Notarangelo L, Ochs HD, Etzioni A *et al*. Cholangiopathy and tumours of the pancreas, liver and biliary tree in boys with X-linked immunodeficiency with hyper-IgM. *J Immunol* 1997; **158**: 977–983.
41 van Mierlo GJ, den Boer AT, Medema JP, van der Voort EI, Fransen MF, Offringa R *et al*. CD40 stimulation leads to effective therapy of CD40(−) tumors through induction of strong systemic cytotoxic T lymphocyte immunity. *Proc Natl Acad Sci USA* 2002; **99**: 5561–5566.
42 French RR, Chan HTC, Tutt AL, Glennie MJ. CD40 antibody evokes a cytotoxic T-cell response that eradicates lymphoma and bypasses T cell help. *Nat Med* 1999; **5**: 548–553.
43 Khanna R, Cooper L, Kienzle N, Moss DJ, Burrows SR, Khanna KK. Engagement of CD40 antigen with soluble CD40 ligand up-regulates peptide transporter expression and restores endogenous processing function in Burkitt's lymphoma cells. *J Immunol* 1997; **159**: 5782–5785.
44 Davies CC, Mason J, Wakelam MJ, Young LS, Eliopoulos AG. Inhibition of phosphatidylinositol 3-kinase- and ERK MAPK-regulated protein synthesis reveals the pro-apoptotic properties of CD40 ligation in carcinoma cells. *J Biol Chem* 2004; **279**: 1010–1019.
45 Haswell LE, Glennie MJ, Al-Shamkhani A. Analysis of the oligomeric requirement for signaling by CD40 using soluble multimeric forms of its ligand, CD154. *Eur J Immunol* 2001; **31**: 3094–3100.
46 Correale P, Aquino A, Giuliani A, Pellegrini M, Micheli L, Cusi MG *et al*. Treatment of colon and breast carcinoma cells with 5-fluorouracil enhances expression of carcinoembryonic antigen and susceptibility to HLA-A(*)02.01 restricted, CEA-peptide-specific cytotoxic T cells *in vitro*. *Int J Cancer* 2003; **104**: 437–445.
47 Yang S, Haluska FG. Treatment of melanoma with 5-fluorouracil or dacarbazine *in vitro* sensitizes cells to antigen-specific CTL lysis through perforin/granzyme- and Fas-mediated pathways. *J Immunol* 2004; **172**: 4599–4608.
48 Apetoh L, Ghiringhelli F, Tesniere A, Obeid M, Ortiz C, Criollo A *et al*. Toll-like receptor 4-dependent contribution of the immune system to anticancer chemotherapy and radiotherapy. *Nat Med* 2007; **13**: 1050–1059.